Gating the charge state of single Fe dopants in the topological insulator Bi_2Se_3 with a scanning tunneling microscope

Can-Li Song,[1,2] Ye-Ping Jiang,[1,2] Yi-Lin Wang,[2] Zhi Li,[2] Lili Wang,[2] Ke He,[2] Xi Chen,[1] Xu-Cun Ma,[2,*] and Qi-Kun Xue[1,2,†]

[1]*State Key Laboratory of Low-Dimensional Quantum Physics, Department of Physics, Tsinghua University, Beijing 100084, China*

[2]*State Key Laboratory for Surface Physics, Institute of Physics, Chinese Academy of Sciences, Beijing 100190, China*

(Received 5 April 2012; revised manuscript received 14 June 2012; published 25 July 2012)

Low-temperature scanning tunneling microscope (STM) is exploited to study directly the atomic and electronic structures of single Fe dopants in topological insulator Bi_2Se_3 thin films. Fe atoms predominantly and isovalently substitute for two distinct Bi sites at the subsurface with charge neutrality. In the vicinity of Fe substitutions, circular depressions in STM topography and sharp rings in spatially resolved conductance map, whose diameters apparently depend on the tunneling conditions, are observed. We show that the phenomena correlate well with the switching between Fe^{3+} and Fe^{2+} charge states due to the gate effect of the tunneling tip, as further evidenced by a multidopant system.

DOI: 10.1103/PhysRevB.86.045441 PACS number(s): 73.20.Hb, 68.37.Ef, 73.50.Gr, 85.35.Gv

I. INTRODUCTION

Topological insulators, a new quantum state of matter, exhibit many unusual electronic properties and have recently provoked enormous excitement in condensed matter physics.[1–3] Besides the bulk energy gap, topological insulators embody a metallic Dirac-like surface state protected by time reversal symmetry.[4–6] Perturbations from magnetic dopants in the bulk or on the surface may result in a long-range magnetic order and open an energy gap at the Dirac point,[7,8] with potentials in quantum computation and spintronics. Theoretically it is predicted that a quantized anomalous Hall state can be realized in magnetic topological insulator ultrathin films.[9] From this point of view, atomic-scale characterization of magnetic dopants in topological insulators is crucial for the understanding of these properties. Moreover, the miniaturization of electronic devices in the future also requires full knowledge of single impurities in topological insulator materials.

With its high spatial and energy resolution, scanning tunneling microscopy (STM) proves to be an excellent tool for characterizing single impurities in semiconductors[10–17] and, thus, in topological insulators as well.[18] In addition, analogous to the three-terminal field effect transistor geometry, the scanning tip and vacuum tunnel junction in STM act as a movable gate and the insulating oxide layer, respectively. This enables us to directly examine single impurities under electrical fields, which may provide very useful information on future topological insulator field-effect devices.[19]

In this article, we utilize STM to characterize single Fe dopants in topological insulator Bi_2Se_3 thin films grown by molecular beam epitaxy. Fe atoms appear to either occupy interstitial sites or isovalently substitute for two distinct Bi sites at the subsurface, with the latter dominant. Around Fe substitutions, we observe circular depressions in STM topography and sharp rings in the spatially resolved conductance dI/dV map, respectively, whose diameters critically rely on the tunneling conditions. Reversible switching between Fe^{3+} and Fe^{2+} charge states due to the gate effect of the STM tip is suggested to be responsible for the observed phenomena. This is well justified by performing tip-to-sample separation-dependent conductance spectra as well as multidopant experiments.

II. EXPERIMENT

Our experiments were conducted in a commercial Unisoku ultrahigh-vacuum cryogenic STM apparatus, equipped with a molecular beam epitaxy chamber for *in situ* sample preparation. The base pressure is better than 5×10^{-11} Torr. High-quality Bi_2Se_3 films have been demonstrated previously on a graphitized SiC(0001) substrate.[20] Here the same growth recipes, with a substrate temperature of 220°C and a high Se/Bi beam flux ratio (>10), were borrowed to grow Fe-doped Bi_2Se_3 crystalline thin films. By thermal desorption of silicon at 1300°C, double-layer graphene was formed on SiC(0001) and used as the substrate. High-purity Bi (99.999%) and Se (99.999%) sources (Alfa Aesar) were evaporated from standard Knudsen cells; Fe, from a homemade Ta boat. The film thicknesses studied here are typically 20 quintuple layers (QLs), with a Fe doping concentration of $2.8 \times 10^{19}/\text{cm}^3$ (∼1 per 500 Bi sites). The relatively low doping level allows us to study single Fe dopants, which are not severely disturbed by others. All STM measurements with an electrochemically etched tungsten tip were performed at 4.8 K. Both conductance spectra and maps were acquired using a standard lock-in technique with a bias modulation of 20 mV at 987.5 Hz.

III. RESULTS AND DISCUSSION

Figures 1(a)–1(c) display three constant-current STM topographic images of Fe-doped Bi_2Se_3 films, where the topmost Se atoms are shown as small (yellow) spheres. Threefold symmetric features related to Fe dopants [those shown in Figs. 1(a) and 1(b) appear more often] are clearly visible, which are little accessible in the as-grown Bi_2Se_3 films.[20] To reveal the specific occupation sites of these dopants, Fig. 1(d) presents the rhombohedral crystal structure of Bi_2Se_3 (side view along the [111] direction). Hexagonally arranged Bi or Se atomic planes are closely packed in a face-centered cubic (fcc) fashion. Five planes with a stacking sequence of Se-Bi-Se-Bi-Se form a unique QL. There is a covalent and strong bonding between Bi and Se atoms within a QL, while the interactions between two neighboring QLs appear to be of the weak van der Waals type.[21] This unique feature implies that the observed Fe dopants most likely originate

 ©2012 American Physical Society

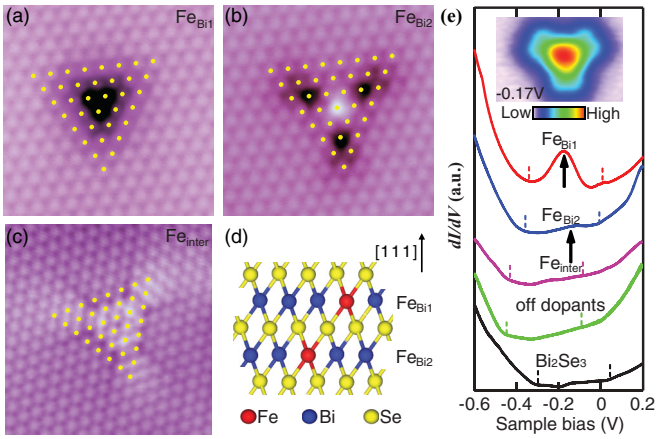

FIG. 1. (Color online) (a)–(c) STM topographies of Fe dopants in the first QL of Bi_2Se_3 films taken at a sample bias V_s of 2 mV. The (yellow) spheres denote the Se atoms in the topmost layer. Image size: (a), (b) 5 nm × 5 nm; (c) 6 nm × 6 nm. (d) Crystal structure of Bi_2Se_3 showing atomic ordering along the rhombohedral [111] direction in a QL. Two Fe substitutions for Bi sites are labeled Fe_{Bi1} and Fe_{Bi2}, respectively. (e) Tunneling spectra on pristine Bi_2Se_3 films, dopant-free regions in Fe-doped Bi_2Se_3 films, and Fe dopants with a fixed tip-to-sample separation ($V_s = 0.2$ V, $I = 0.2$ nA). Dashes show the onset of conduction and valence bands. Inset: dI/dV map at −0.17 eV (3 nm × 2 nm) around Fe_{Bi1} dopant.

from the first QL close to the Bi_2Se_3 top surface, leaving the deeper ones unattainable for STM. Moreover, we note that both dopants in Figs. 1(a) and 1(b) dramatically disturb the electronic density of states (DOS) with three depressions on the surface. Phenomenologically, they are in quite good agreement with Fe substitutions. The Fe atoms in Fig. 1(c) seem to occupy the interstitial sites since they perturb the electronic states weakly. Together with the spatial extent and position of three Fe dopants, we suggest here that the Fe atoms shown in Figs. 1(a) and 1(b) substitute at Bi sites two and four atomic layers below the surface, while those in Fig. 1(c) occupy interstitial sites. For convenience, we hereafter refer to them as Fe_{Bi1}, Fe_{Bi2}, and Fe_{inter}, respectively. The predominance of Fe_{Bi} substitutions shows that Bi substitutional sites are the most energetically favorable sites for single Fe dopants in Bi_2Se_3, quite in line with the recent theoretical prediction.[22]

Further evidence from differential conductance (dI/dV) spectra measurements corroborates the above interpretation. Figure 1(e) depicts a series of dI/dV spectra on as-grown Bi_2Se_3 films, Fe-doped Bi_2Se_3 films, and three types of Fe dopants. The vertical dashes indicate the valence and conduction band edges of Bi_2Se_3. As expected, Fe interstitials dope electrons and shift the bands downward (>130 mV; magenta and green lines). In the near vicinity of Fe_{Bi1} and Fe_{Bi2}, the bands move upward with respect to other regions in Fe-doped Bi_2Se_3 films, signifying local hole doping. However, this does not mean that Fe substitutes for Bi as the Fe^{2+} state and resembles the aliovalent Ca^{2+} and Mn^{2+} acceptors in Bi_2Se_3 and Bi_2Te_3 single crystals.[23,24] On the contrary, Fe indeed substitutes for Bi as the Fe^{3+} state at equilibrium. Otherwise, the hole-doping effect of Fe^{2+} dominates and thus wholly shifts the band upward, inconsistent with our observation [green line in Fig. 1(e)]. This apparent discrepancy originates from the gate effect of an STM tip, as detailed below.

Moreover, dI/dV spectra on Fe_{Bi1} and also, possibly, Fe_{Bi2} show broad peaks at $V_{peak} \sim -0.17$ V (arrows) within the band gap, not at the band edges where the shallow donor or acceptor states should be located. We attribute the observed peaks to Fe dopant levels (D), and their broadening may be due to their resonances with the surface state within the gap of the Bi_2Se_3 topological insulator.[4–6] Previous studies have shown that the dopant level hybridizes with the host and a spectroscopic image of the resonant-state wave function can reflect the host symmetry.[14] This image, shown in the inset in Fig. 1(e), indeed reveals that the Fe_{Bi1} resonance state exhibits an anisotropic triangular-shaped structure, in good consistency with the rhombohedral crystal structure of Bi_2Se_3.

Intriguingly, around each Fe substitution, we observe dusky disk-like features extending several nanometers below a specific sample voltage, as shown in Figs. 2(a) and 2(b) (only Fe_{Bi1} dopant shown). The disks do not disturb the topmost Se atomic corrugation, but the diameter changes with the applied sample voltage. With other experimental conditions fixed, a higher bias voltage leads to a smaller disk. In the spatially resolved differential conductance map with the feedback loop open, the edge of each disk appears as a sharp ring with the narrow width of ∼0.5 nm [Fig. 2(c)]. The diameter of the ring depends on the applied voltage as well, in the same manner. This is more clearly demonstrated in Fig. 2(d), which depicts a cross-sectional view of the differential conductance running

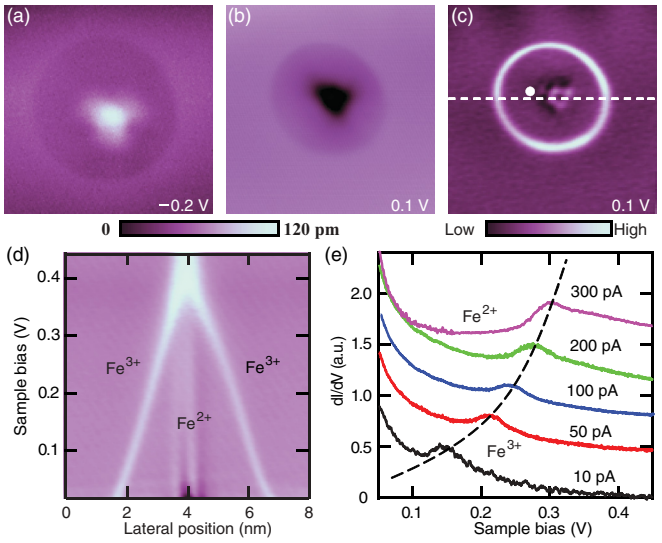

FIG. 2. (Color online) (a), (b) STM topographies (8 nm × 8 nm) of Fe_{Bi1} dopant taken at a tunneling current of 0.2 nA and sample biases of (a) −0.2 V and (b) 0.1 V. Lower topographic contrast is discernible in the vicinity of the dopant. (c) Spatially resolved dI/dV map (8 nm × 8 nm) with the feedback loop open ($V_s = 0.1$ V, $I = 0.2$ nA). The sharp ring with enhanced differential conductance corresponds to the edge of the dark disk in (b). (d) dI/dV cross section along the dashed line in (c). The bright features represent the position of the ring. (e) A series of dI/dV spectra with the feedback on at the white circle in (c). The peak shifts monotonically toward a higher voltage with the tunneling current setpoint. Dashed (black) curve is a guide for the eye.

through the dopant position [dashes in Fig. 2(c)]. The two bright lines with enhanced dI/dV values show the positions of the ring as a function of the sample bias voltage, and their horizontal separation represents the ring diameter. Clearly, the diameter shrinks with the voltage until the ring disappears at ~0.4 eV. Furthermore, it is found that the ring size varies with the tip-to-sample separation. A smaller separation invariably results in a larger ring. These observations suggest that the above phenomena do not correlate with the local electronic DOS effects. This is unambiguously confirmed by a series of dI/dV spectra at various tunneling current setpoints [Fig. 2(e)]. With increasing setpoint, a monotonic upward shift of the pronounced peak (switching between Fe^{2+} and Fe^{3+} charge states, with details below) is discernible. This clearly rules out the local DOS scenario, where the peak energy is never expected to alter with the current setpoint.

Previously, similar features were observed in the vicinity of single subsurface dopants in semiconductors (e.g., GaAs and InAs),[10–13,15,16] an alkali-metal-doped C_{60} complex,[25] and cobalt adatoms on graphene.[26] They are explained as the switching of the dopants' charge state due to tip-induced band bending (TIBB). The switch occurs at a specific threshold value of TIBB, where the dopant level crosses the bulk Fermi level or band edges. The TIBB and thus the charge switching depend on the tunneling conditions, tip termination, and carrier density of the substrate. The resultant change in the dopants' electrostatic field affects the local band structure of the host underneath the tip and, consequently, leads to the observed disklike feature in STM topography and ring in the conductance map. In the Fe-doped Bi_2Se_3 topological insulator with a bulk band gap, given the low carrier density of surface states, the mechanism remains the same. In our case, the dopant level is located well below the Fermi energy and conduction band edge [Fig. 1(e)]. To achieve their crossings with the dopant level, one has to apply an extremely high positive voltage and bend the dopant level upward. Accordingly, the size of the disk or ring should increase with the applied bias voltage, in sharp contrast to our observation. Therefore, the observed disks or rings around subsurface Fe in Bi_2Se_3 cannot be understood as the crossing of the dopant level with either the bulk Fermi level or the conduction band.

We thus suggest an alternative model, the crossing between the dopant level and the bulk valence band, as illustrated schematically in Fig. 3. As the STM tip is laterally far away from the Fe dopant (Fe^{3+}), the electronic bands around the dopant remain undisturbed and always flat. However, when the tip approaches the Fe_{Bi} dopant and the sample voltage deviates from the flat-band voltage V_{FB},[10] the bands around the Fe_{Bi} dopant will be perturbed due to the gate effect of the STM tip [Figs. 3(a) and 3(b)]. Specifically, it causes electrons to accumulate underneath the tip below the V_{FB}. In terms of the ultrasharp tips we used, the accumulation region extends laterally for only a few nanometers. At the same time, the bands and dopant level bend downward, as displayed in Figs. 3(b) (bottom panel) and 3(c). As the dopant level lowers to the onset of the valence band in the bulk [Fig. 3(c)], the electron will tunnel from the valence band into the Fe_{Bi} dopant and thus ionize Fe^{3+} into Fe^{2+}. The resultant Coulomb potential of Fe^{2+} lifts the bands around the dopant

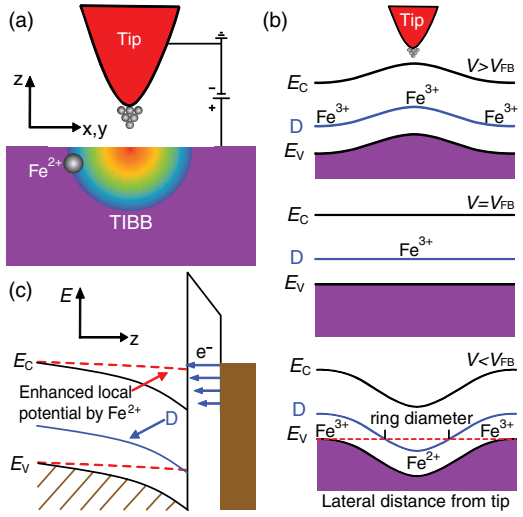

FIG. 3. (Color online) Schematic showing the switching mechanism of Fe charge states. (a) Band perturbation around Fe_{Bi} dopant due to the gate effect of the STM tip. (b) Lateral TIBB below the STM tip for various sample voltages. Bottom panel: The separation between the two vertical lines indicates the diameter of the sharp conductance ring in Fig. 2(c). (c) Band lifting (red dashes) by the Fe^{2+} state.

(red dashes) in Fig. 3(c)], thereby reducing the number of states available for electron tunneling. The tunneling current is instantaneously reduced, leading to an approach of the tip. This process can be visible as dusky disks in topographic images [Figs. 2(a) and 2(b)], a ring structure in the dI/dV map [Fig. 2(c)], and pronounced peaks in the dI/dV spectra [Fig. 2(e)]. The present model predicts larger disks or rings for a smaller sample bias and small tip-sample separation (large TIBB) as well as an upward shift of the dI/dV peak with the current setpoint, as observed in our experiments. Finally, as the STM tip is located on any Fe_{Bi} substitution, the TIBB immediately electrifies the Fe^{3+} and so locally lifts the band. This explains the dI/dV spectra on Fe_{Bi} substitutions in Fig. 1(e) well.

The proposed model is further supported by studying a multidopant system with small interdopant separation (<5 nm), where ionization exhibits a more complex behavior. Figure 4(a) shows such a dI/dV map around three Fe_{Bi1}

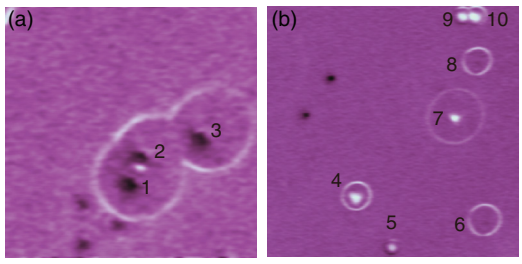

FIG. 4. (Color online) (a) Differential conductance dI/dV map (15 nm × 15 nm, $V_s = 0.1$ V, $I = 0.2$ nA) around three Fe_{Bi1} dopants. (b) Large-scale dI/dV map (30 nm × 30 nm, $V_s = -0.1$ V, $I = 0.2$ nA) with coexisting Fe_{Bi1} (4, 5, 7, 9, and 10) and Fe_{Bi2} (6 and 8) dopants. The two dark-hole features at the top left correspond to Se vacancies.[20]

dopants. Evidently, bright features between a pair of overlap rings either disappear (dopants 2 and 3) or change into another bright slice (dopants 1 and 2). They are due to the electrostatic interactions between the neighboring dopants.[27] As a Fe dopant is reduced to the Fe^{2+} state, it will lift the surrounding bands and thus increase the ionization threshold for the neighboring Fe dopant. As such, a lower voltage (namely, a larger TIBB) is needed to switch the second Fe^{3+} dopant, which actually causes the above-mentioned features. A previous study has also demonstrated that the size of the ionization ring depends critically on the dopant depth[13] and that the ring size is almost the same for all dopants with an identical depth. This differs from our findings. As shown in Fig. 4(b), the ring diameter around Fe_{Bi1} dopants (labeled 4, 5, 7, 9, and 10) differs by 4, despite identical experimental conditions. Near-surface defect-induced band bending may change the band configuration around Fe dopants and then the ring diameter.[15,16] However, this does not apply in our case, where little defect is found around the studied dopants. Meanwhile, Fe interstitials show little correlation with the ring diameter. Instead we suggest that the nanoscale spatial inhomogeneity in DOS, probably caused by Fe doping,[28] can qualitatively account for our observations. A high local DOS often weakens the TIBB and leads to a small ring there.

IV. SUMMARY

In summary, we have investigated Fe-doped Bi_2Se_3 films by STM. Most Fe atoms substitute for Bi sites in the Fe^{3+} state. We show that Fe^{3+} substitution ion can be switched into Fe^{2+} with an STM tip in a controlled manner. The switching depends critically on the specific experimental conditions and environments around Fe^{3+} ions. The present study sheds new insights on the route to future topological insulator device applications.

ACKNOWLEDGMENTS

This work was supported by the National Science Foundation and Ministry of Science and Technology of China. All STM topographic images were processed by WSxM software (www.nanotec.es).

*Corresponding author: xcma@aphy.iphy.ac.cn
†qkxue@mail.tsinghua.edu.cn

[1] X. L. Qi and S. C. Zhang, Phys. Today **63**(1), 33 (2010).
[2] J. E. Moore, Nature **464**, 194 (2010).
[3] M. Z. Hasan and C. L. Kane, Rev. Mod. Phys. **82**, 3045 (2010).
[4] P. Roushan, J. Seo, C. V. Parker, Y. S. Hor, D. Hsieh, D. Qian, A. Richardella, M. Z. Hasan, R. J. Cava, and A. Yazdani, Nature **460**, 1106 (2009).
[5] T. Zhang, P. Cheng, X. Chen, J. F. Jia, X. C. Ma, K. He, L. L. Wang, H. J. Zhang, X. Dai, Z. Fang, X. C. Xie, and Q. K. Xue, Phys. Rev. Lett. **103**, 266803 (2009).
[6] J. Seo, P. Roushan, H. Beidenkopf, Y. S. Hor, R. J. Cava, and A. Yazdani, Nature **466**, 343 (2010).
[7] Y. L. Chen, J. H. Chu, J. G. Analytis, Z. K. Liu, K. Igarashi, H. H. Kuo, X. L. Qi, S. K. Mo, R. G. Moore, D. H. Lu, M. Hashimoto, T. Sasagawa, S. C. Zhang, Z. Fisher, I. R. Hussain, and Z. X. Shen, Science **329**, 659 (2010).
[8] L. A. Wray, S. Y. Xu, Y. Xia, D. Hsieh, A. V. Fedorov, Y. San Hor, R. J. Cava, A. Bansil, H. Lin, and M. Z. Hasan, Nat. Phys. **7**, 32 (2010).
[9] R. Yu, W. Zhang, H. J. Zhang, S. C. Zhang, X. Dai, and Z. Fang, Science **329**, 61 (2010).
[10] F. Marczinowski, J. Wiebe, J. Tang, M. Flatte, F. Meier, M. Morgenstern, and R. Wiesendanger, Phys. Rev. Lett. **99**, 157202 (2007).
[11] F. Marczinowski, J. Wiebe, F. Meier, K. Hashimoto, and R. Wiesendanger, Phys. Rev. B **77**, 115318 (2008).
[12] K. Teichmann, M. Wenderoth, S. Loth, R. G. Ulbrich, J. K. Garleff, A. P. Wijnheijmer, and P. M. Koenraad, Phys. Rev. Lett. **101**, 076103 (2008).
[13] A. P. Wijnheijmer, J. K. Garleff, K. Teichmann, M. Wenderoth, S. Loth, R. G. Ulbrich, P. A. Maksym, M. Roy, and P. M. Koenraad, Phys. Rev. Lett. **102**, 166101 (2009).
[14] A. Richardella, D. Kitchen, and A. Yazdani, Phys. Rev. B **80**, 045318 (2009).
[15] D. H. Lee and J. A. Gupta, Science **330**, 1807 (2010).
[16] D. H. Lee and J. A. Gupta, Nano Lett. **11**, 2004 (2011).
[17] P. M. Koenraad and M. E. Flatté, Nat. Mater. **10**, 91 (2011).
[18] D. West, Y. Y. Sun, S. B. Zhang, T. Zhang, X. C. Ma, P. Cheng, Y. Y. Zhang, X. Chen, J. F. Jia, and Q. K. Xue, Phys. Rev. B **85**, 081305 (2012).
[19] F. Xiu, L. He, Y. Wang, L. Cheng, L. T. Chang, M. Lang, G. Huang, X. F. Kou, Y. Zhou, X. W. Jiang, Z. G. Chen, J. Zou, A. Shailos, and K. L. Wang, Nat. Nanotech. **6**, 216 (2011).
[20] C. L. Song, Y. L. Wang, Y. P. Jiang, Y. Zhang, C. Z. Chang, L. L. Wang, K. He, X. Chen, J. F. Jia, Y. Y. Wang, Z. Fang, X. Dai, X. C. Xie, X. L. Qi, S. C. Zhang, X. Q. Xue, and X. C. Ma, Appl. Phys. Lett. **97**, 143118 (2010).
[21] S. Urazhdin, D. Bilc, S. D. Mahanti, S. H. Tessmer, T. Kyratsi, and M. G. Kanatzidis, Phys. Rev. B **69**, 085313 (2004).
[22] J. M. Zhang, W. G. Zhu, Y. Zhang, D. Xiao, and Y. G. Yao, arXiv:1205.3936.
[23] Y. S. Hor, A. Richardella, P. Roushan, Y. Xia, J. G. Checkelsky, A. Yazdani, M. Z. Hasan, N. P. Ong, and R. J. Cava, Phys. Rev. B **79**, 195208 (2009).
[24] Y. S. Hor, P. Roushan, H. Beidenkopf, J. Seo, D. Qu, J. G. Checkelsky, L. A. Wray, D. Hsieh, Y. Xia, S. Y. Xu, D. Qian, M. Z. Hasan, N. P. Ong, A. Yazdani, and R. J. Cava, Phys. Rev. B **81**, 195203 (2010).
[25] N. A. Pradhan, N. Liu, C. Silien, and W. Ho, Phys. Rev. Lett. **94**, 076801 (2005).
[26] V. W. Brar, R. Decker, H. M. Solowan, Y. Wang, L. Maserati, K. T. Chan, H. Lee, Ç. Girit, A. Zettl, S. G. Louie, M. L. Cohen, and M. F. Crommie, Nat. Phys. **7**, 43 (2010).
[27] K. Teichmann, M. Wenderoth, S. Loth, J. K. Garleff, A. P. Wijnheijmer, P. M. Koenraad, and R. G. Ulbrich, Nano Lett. **11**, 3538 (2011).
[28] H. Beidenkopf, P. Roushan, J. Seo, L. Gorman, I. Drozdov, Y. San Hor, R. J. Cava, and A. Yazdani, Nat. Phys. **7**, 939 (2011).